

Autophagy, apoptosis and organelle features during cell exposure to cadmium

CRISTIANE DOS SANTOS VERGILIO AND EDÉSIO JOSÉ TENÓRIO DE MELO*

Universidade Estadual do Norte Fluminense, Centro de Biociências e Biotecnologia, Laboratório de Biologia Celular e Tecidual, Campos dos Goytacazes, RJ, Brasil, 28013-602.

Key words: Cd, cell death, hepatocyte, HuH-7 cells, mitochondria

ABSTRACT: Cadmium (Cd) induces several effects in different tissues, but our knowledge of the toxic effects on organelles is insufficient. To observe the progression of Cd effects on organelle structure and function, HuH-7 cells (human hepatic carcinoma cell line) were exposed to CdCl₂ in increasing concentrations (1 μM – 20 μM) and exposure times (2 h – 24 h). During Cd treatment, the cells exhibited a progressive decrease in viability that was both time- and dose-dependent. Cd treated cells displayed progressive morphological changes that included cytoplasm retraction and nuclear condensation preceding a total loss of cell adhesion. Treatment with 10 μM for 12 h led to irreversible damages. Before these drastic and irreparable damages, treated cells (5 μM for 12 h) presented a progressive loss of mitochondrial function and cytoplasm acidification as well as dysfunction and disorganization of microfilaments and endoplasmic reticulum. These damages led to the induction of apoptotic events and an increase in autophagic bodies in the cytoplasm. These results revealed that Cd affects multiple intra-cellular targets that induce alterations in the mitochondria, cytoskeleton, endoplasmic reticulum and acidic compartments, ultimately culminating in cell death via apoptotic and autophagic pathways.

Introduction

Cadmium (Cd) is a highly toxic metal that exerts multiple effects on organisms (Filipič, 2012; Waisberg *et al.*, 2003; Bertin and Averbeck, 2006). However, the complexity and diversity of events associated with cell-Cd interactions have resulted in fragmented information mainly related with organelle structure and function (Cannino *et al.*, 2009).

Biochemical studies have shown the involvement of organelles (mitochondria, lysosomes and cytoskeleton)

in Cd toxicity in several cell lines (Cannino *et al.*, 2009; Fotakis *et al.*, 2005; Faverney *et al.*, 2004; L'Azou *et al.*, 2002). However, the wide-ranging effects of this metal on organelles and their involvement in induced cell death remain to be fully understood (Fabbri *et al.*, 2012). Therefore, the overall understanding of Cd induced cell damage and toxicity needs the observation of its effects on different intra-cellular targets.

Cd exposure in organisms is followed by injuries in the liver, testes, lungs, kidneys and bones (Ye *et al.*, 2007; Joseph, 2009; Nordberg, 2009; Siu *et al.*, 2009). Cd uptake by hepatocytes makes the liver one of the major sites of Cd accumulation (Fabbri *et al.*, 2012) and reduces its availability to other organs (Souza *et al.*, 1997). Therefore, studies of hepatocyte organelles may help understanding the progression from the direct effects of Cd to its ultimate toxicity.

*Address correspondence to: Edésio José Tenório de MELO.
E-mail: ejtm1202@gmail.com
Received: April 10, 2013. Revised version received: August 13, 2013.
Accepted: August 18, 2013.

With this purpose, the structure and function of mitochondria, acidic organelles and vesicles, endoplasmic reticulum elements and microfilaments was assessed in HuH-7 cells (a human hepatic carcinoma cell line) to observe the progression of Cd toxicity.

Materials and Methods

Cell culture and treatments

HuH-7 cells were maintained in 25 mL cell culture flasks with Dulbecco's Modified Eagle's Medium (DMEM-1152, Sigma Aldrich®) supplemented with 10% fetal bovine serum (Gibco®) in a humidified atmosphere containing 5% CO₂ at 37°C. For experimental purposes, the cells were seeded onto 24-well plastic plates. The optimum cell concentration determined from cell line growth profiles was 10⁵ cells/mL. Cells were allowed to attach for 24 h before Cd treatments.

For Cd toxicity assays, stock solutions (0.1 M CdCl₂) were prepared using ultra-pure quality water, and dilutions were made with culture medium to 1 μM, 5 μM, 10 μM, 15 μM and 20 μM final concentrations. To observe the progression of Cd induced toxic effects, these concentrations were added to cell cultures for 2, 6, 12 and 24 h.

Quantification and morphological analysis of Cd induced toxic effects

Control and Cd exposed cells were fixed in Bouin's solution and stained with Giemsa (10%) for light mi-

croscopy observation. All preparations were examined using a Zeiss Axioplan photomicroscope equipped with 20x and 40x objectives. HuH-7 cell survival was determined by counting the number of living cells in a given area (the cell spread on the substrate and nuclear condensation were considered for discrimination between live and dead cells). For each sample, 6 randomly chosen fields were scored at a magnification of 400x, and results were expressed as the mean ± standard deviation. HuH-7 control cell numbers counted at each time point were considered to be 100%. Digital images were obtained using an Axioplan microscope equipped with a Canon Power Shot camera A610/620 employing 20x and 40x objectives.

Cell viability analysis with MTT assay

Following exposure to Cd, the cells were incubated with MTT (3-(4,5-dimethylthiazol-2-yl)-2,5-diphenyltetrazolium bromide, 6 mg/mL) in culture medium for 4 h at 37°C (Mosmann, 1983). After the removal of MTT-containing medium, 200 μL of DMSO (dimethylsulfoxide) were added, and the absorbance at 540 nm was measured after 5 min in a microplate reader (Thermoplate© TP reader). Results were expressed as mean ± standard deviation of triplicate experiments.

Scanning and transmission electron microscopy (SEM and TEM)

HuH-7 cells treated with 5 μM CdCl₂ for 12 h were fixed in 2.5% (v/v) glutaraldehyde and 4% (v/v) formaldehyde in 0.1 M cacodylate buffer (pH 7.2). For

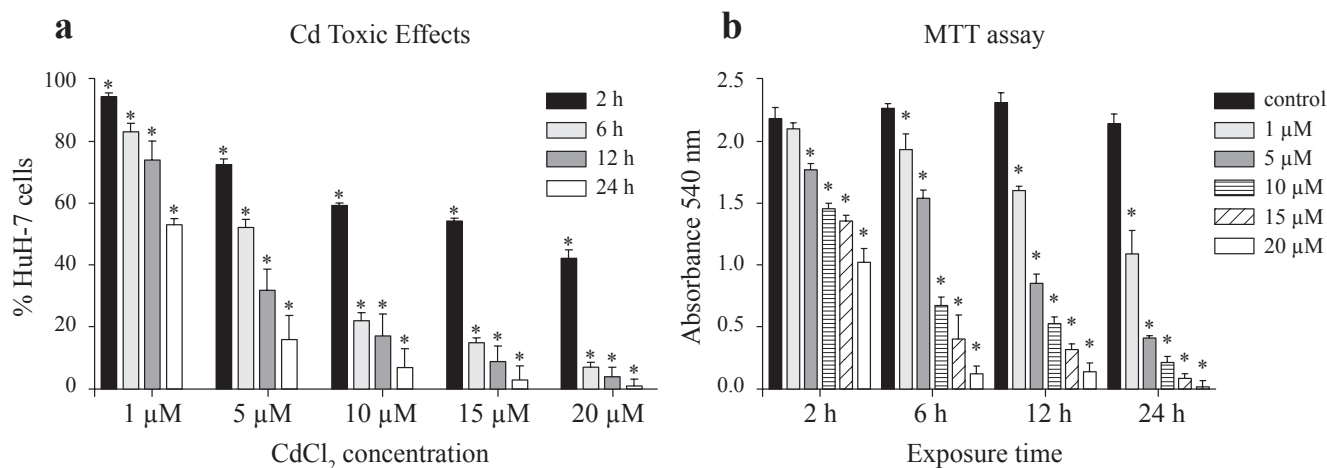


FIGURE 1. CdCl₂ toxic effects on viability of HuH-7 cells. (a) Quantification of Giemsa stained HuH-7 cells after CdCl₂ treatment. All concentrations tested were compared to a control group that was defined as 100%. (b) Decrease in cell viability by MTT assay in a dose/time dependent manner. *Significantly different from control ($p < 0.001$).

SEM preparations, the samples were washed, dehydrated with a graded series of ethanol, critical-point dried in CO₂, positioned on a specimen holder and sputtered with gold. All micrographs were recorded using a Zeiss Evo 40 microscope employing secondary electrons. For TEM, the fixed samples were post-fixed with (1:1) 1% osmium tetroxide and 0.8% potassium ferricyanide, dehydrated with acetone and embedded in Epon. Ultra-thin slices (70 nm) were obtained with a Leica Reichert Ultracut S ultramicrotome, contrasted with uranyl acetate (5%) and lead citrate and observed using a Zeiss 900 transmission electron microscope.

Reversibility of Cd induced toxic effects

For reversibility testing, HuH-7 cells were incubated for 6 h with 10 μM or 20 μM CdCl₂ or for 12 h with 5 μM or 10 μM of CdCl₂. After exposure, the cells were washed and the medium was replaced without Cd addition. After a 24 h recovery period, cells were analysed by light microscopy and quantified as described above.

Fluorescence analyses

For assessment of mitochondrial function, control and Cd exposed HuH-7 cells were incubated with Rhodamine 123 (10 μg/mL) (Sigma Aldrich®) for 30 min in 5% CO₂ at 37°C (Johnson *et al.*, 1980). To observe acidic organelles and compartments, control and Cd treated cultures were incubated with acridine orange (5 μg/mL) (Sigma Aldrich®) for 40 min in a 5% CO₂ incubator at 37°C (Kielian and Cohn, 1980). Lysosomes were stained with LysoTracker Red (Molecular Probes®) (50 nM) added to the HuH-7 cultures in cell medium without fetal bovine serum for 30 min at 37°C. Rhodamine phalloidin (Molecular Probes®) and DiOC₆ (Sigma Aldrich®) were used to observe F-actin (a major component of the cytoskeleton) and the endoplasmic reticulum, respectively, and were added to formaldehyde-fixed control and Cd exposed HuH-7 cells. Rhodamine phalloidin (200 units/mL) was added to cell cultures for 40 min (Barak *et al.*, 1980), and DiOC₆ (2.5 μg/mL) was incubated with cells for 10 min (Terasaki *et al.*, 1984).

Given that only apoptotic cells will take up YO-PRO-1 and viable cells exclude the dye, YO-PRO-1 dye was used (Molecular Probes®) for detection of apoptosis (Idziorek *et al.*, 1995; Plantin-Carrenard *et al.*, 2003). YO-PRO-1 (1 μM) was added to HuH-7 cell cultures for 30 min in an incubator with 5% CO₂ at 37°C.

For autophagic vacuole detection, a selective marker monodansylcadaverine (MDC) (Sigma Aldrich®) was used as described by Biederbick *et al.* (1995). The cell

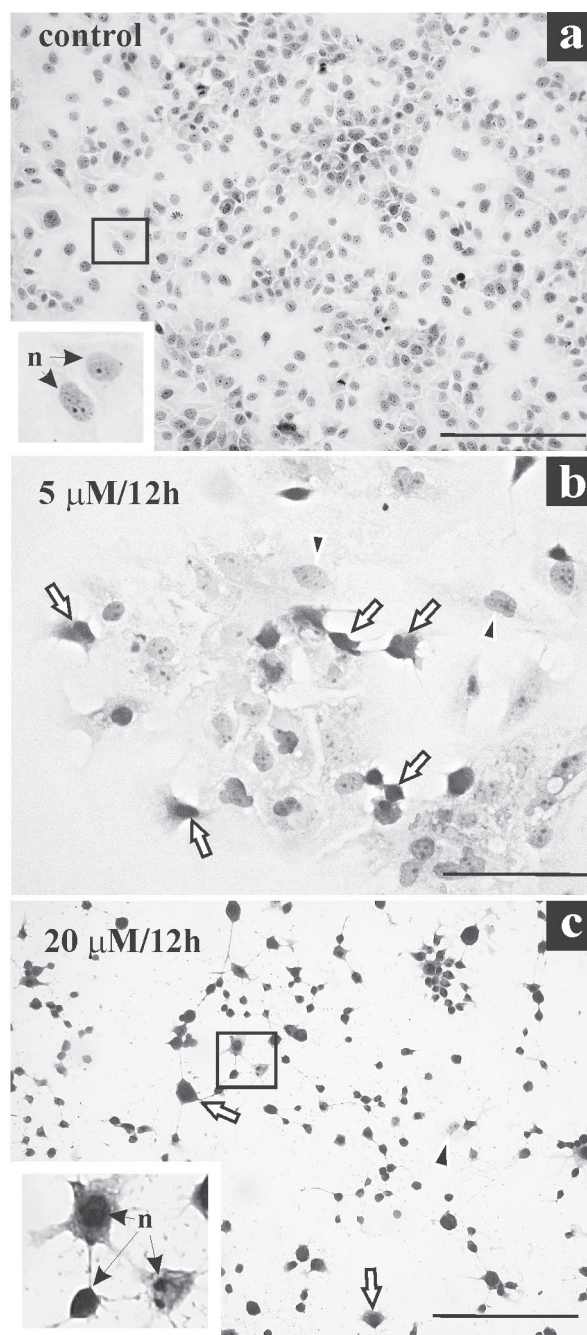


FIGURE 2. Light microscopy of HuH-7 cells showing morphological alterations induced by CdCl₂. (a) Control cells in monolayer. (b) Changes in the cell monolayer following incubation with 5 μM for 12 h. (c) Complete cell detachment after incubation with 20 μM for 12 h. (b) and (c) also show treated cells with retraction and nuclear condensation (arrows). Cells displaying normal morphology are also seen (arrowheads). n = nucleus. Scale bars: A and C: 200 μm; B: 100 μm.

culture was incubated with 0.05 mM MDC in PBS at 37°C for 10 min.

All the stained cells were observed under a Zeiss Confocal Laser Scan Microscope (CLSM) using a 543 nm argon laser and a 40x objective.

Statistical analyses

All data are expressed as the means \pm standard errors. Statistical analyses were made using GraphPad Prism v.4 software (GraphPad Software, Inc. CA,

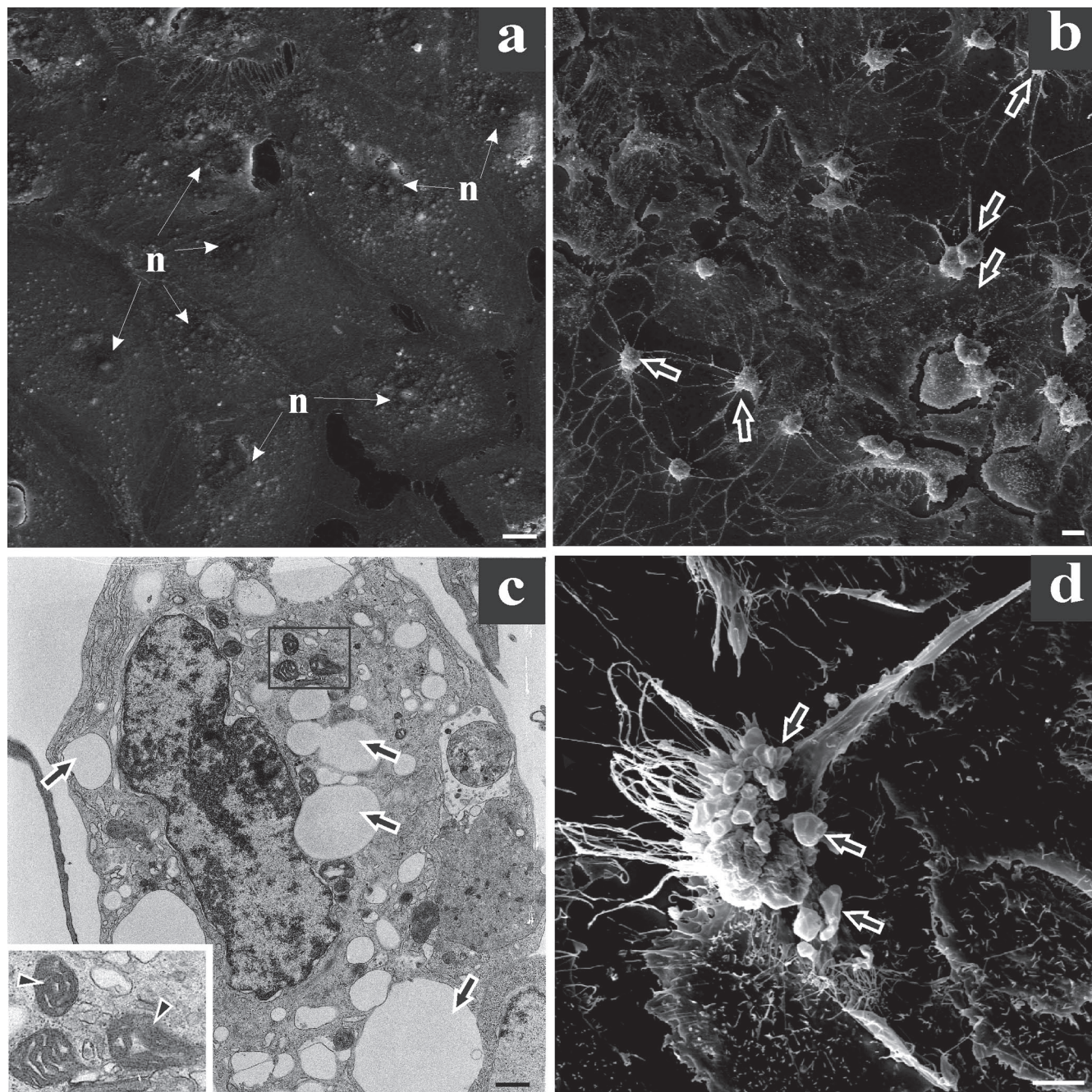


FIGURE 3. Scanning (a, b, d) and transmission (c) electron microscopy showing HuH-7 cell cultures before (a) and after Cd treatment (b - d) (5 μ M for 12 h). (a) Characteristic aspect of control monolayer. (b) Presence of many detaching rounded cells (arrows). (c) Ultra-structural appearance of Cd treated cells with many vacuoles in the cytoplasm (arrows) and the collapse of some mitochondrial cristae (inset, arrowheads). (d) Cells with membrane blebs (arrows) following Cd treatment. n = nucleus. Scale bar: A: 20 μ m, B: 20 μ m, C: 1.1 μ m, D: 10 μ m.

USA). The two-way analysis of variance followed by the Bonferroni test was performed for cell viability data and reversibility test data. Differences were considered significant when $p < 0.05$.

Results

To determine the threshold of metal damage and its relationship to metal toxicity (induction of cell death), the present study investigated the effects of Cd over the HuH-7 cell machinery after treatments with increasing concentrations and exposure times.

The dose and duration of treatment were critical factors in the induction of cell death (Fig. 1a). These toxic effects were evaluated after each Cd treatment following the observation of reduced cell numbers demonstrated by the attached cell count (Fig. 1a). Cell viability was assessed through the MTT assay, verifying the decrease of cell viability indicated by the failure of mitochondrial function (Fig. 1b). The results obtained by counting the surviving cells or through assessment of mitochondrial function by MTT assay corroborate the Cd toxicity in the culture.

The observation of the Cd induced toxic effects indicated that healthy cells at semi-confluence, evidenced by adherence and spread cytoplasm on the substrate with prominent nuclei and nucleoli, changed during Cd treatment (Fig. 2a, 2b). Cells experienced different degrees of cytoplasm shrinkage and nuclear condensation (Fig. 2b). This cytoplasmic retraction was more evident at higher doses (20 μM), but occurred asynchronously within the culture (Fig. 2c, inset) and led to the gradual loss of cell viability and subsequent release from the substrate.

Ultrastructural analysis of cell culture indicated that cell morphology (Fig. 3a) changed in the presence of Cd (5 μM for 12 h) as evidenced by cytoplasm retraction (Fig. 3b), severe vacuolization (Fig. 3c, arrows) and alterations in mitochondrial structure (Fig. 3c, inset). The presence of blebs on the membrane cell surface (Fig. 3d, arrows) also indicated apoptosis, and this was also confirmed by YO-PRO-1 nuclear staining (Fig. 4a- d). No indicative probe (Fig. 4b, arrowhead) was observed in the adherent control cells (Fig. 4a). However, following Cd exposure (5 μM for 12 h), staining was evident in cells with cytoplasmic retraction and nuclear disorganisation (Fig. 4c, d, arrowheads). The cells displayed different stages of cellular retraction (Fig. 4c) with distinct apoptotic staining (Fig. 4d), suggesting that the process occurred asynchronously within the same culture.

To assess the reversibility of Cd induced damage, cells were treated with 5 and 10 μM CdCl₂ for 12 h or with 10 and 20 μM CdCl₂ for 6 h, and then maintained in the absence of Cd for 24 h. After Cd removal, both treatments (10 and 20 μM) for the short period (6 h) and the lower concentration (5 μM) with long-term exposure (12 h) the culture was able to recover (Fig. 5a-h). However, treatment with 10 μM for 12 h promoted severe deleterious changes (Fig. 5i, j) that compromised cellular recovery (Fig. 5b). This finding is important to understand the kinetics of metal action on the cellular machinery.

The treatment with 5 μM for 12 h was chosen to investigate the Cd induced changes in organelles and severe damages that compromised cell survival were observed. Initially, organelle functionality was analysed using the mitochondrial fluorescent stain Rhodamine 123 (Fig. 6a-d). The intense and spread filaments indicative of functional mitochondria (Fig. 6b, arrowheads) present in control cells changed to punctate staining

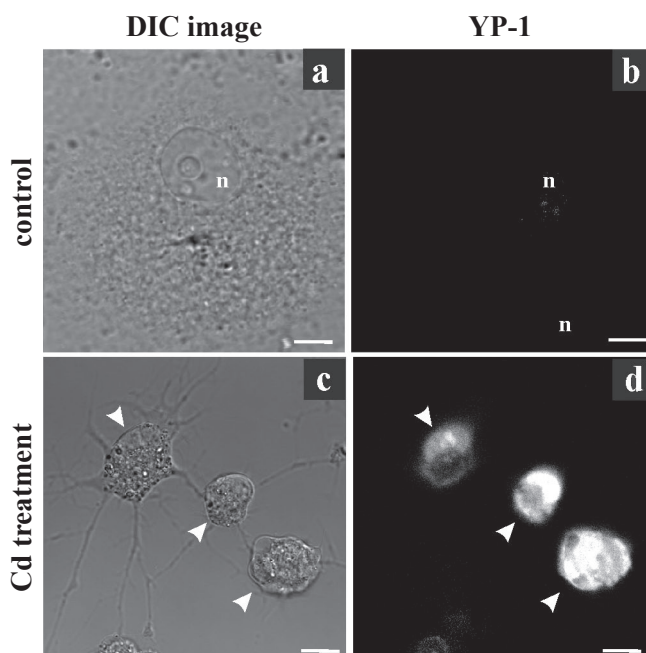


FIGURE 4. Differential interference contrast microscopy (DIC) (a and c) and confocal laser scanning microscopy of HuH-7 cells stained with YO-PRO-1 (YP-1) (1 μM) (b and d) before (a and b) and after Cd treatment with 5 μM for 12 h (c and d). (a) Control cells. (b) No fluorescence signal in untreated cell. (c) Differential levels of cytoplasm retraction and nuclear disorganisation, both characteristics of apoptotic processes observed in Cd treated cells. (d) Cellular staining indicative of cell death via apoptotic processes following CdCl₂ exposure. n= nucleus. Scale bar: 10 μm .

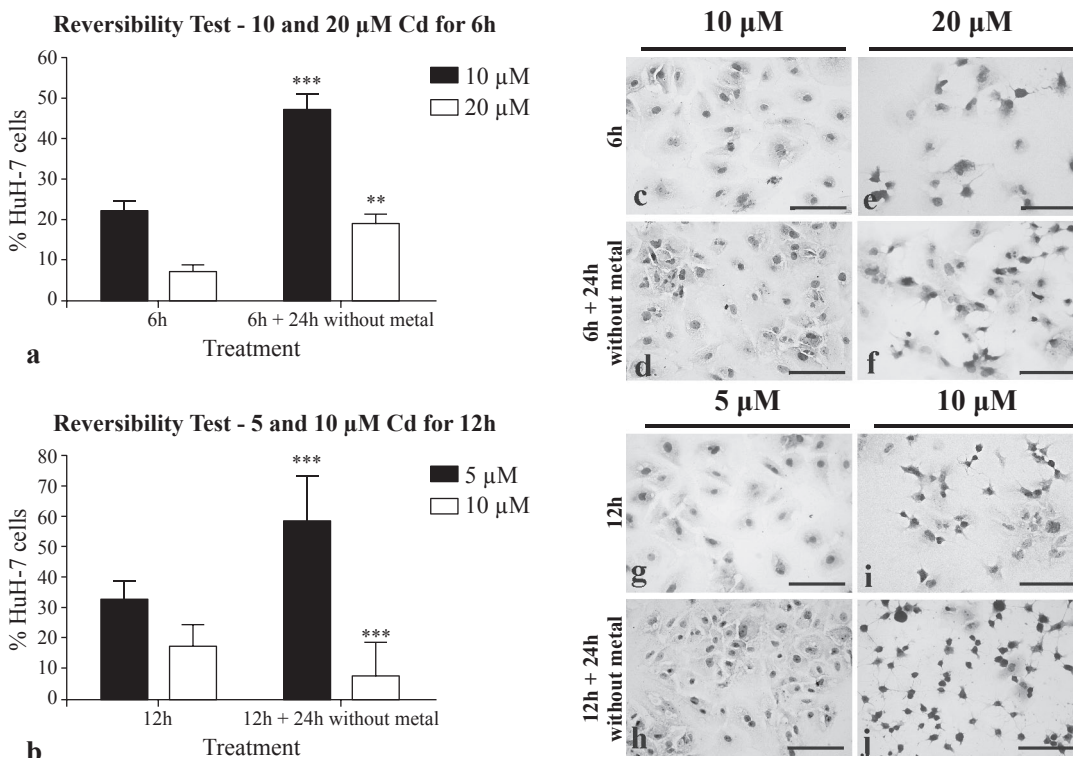


FIGURE 5. Reversibility of Cd effects on HuH-7 cells. (a) Recovery in culture after 24 h of Cd removal following the treatments with higher concentrations and short exposure time (10 μM and 20 μM for 6 h). (b) Recovery of culture following long-term exposure (12 h) with 5 μM with subsequent 24 h of Cd removal. However, the same capability to reverse Cd toxicity was not observed after 12 h incubation with 10 μM ; where the toxic effects last even after Cd removal. (c - j) Morphological aspects of the culture following each Cd treatment: (c) 10 μM for 6 h, (d) 10 μM for 6 h + 24 h without Cd, (e) 20 μM for 6 h, (f) 20 μM for 6 h + 24 h without Cd, (g) 5 μM for 12 h, (h) 5 μM for 12 h + 24 h without Cd, (i) 10 μM for 12 h, (j) 10 μM for 12 h + 24 h without Cd. The concentrations tested were compared with a control group that was considered 100%. *** $p < 0.001$.

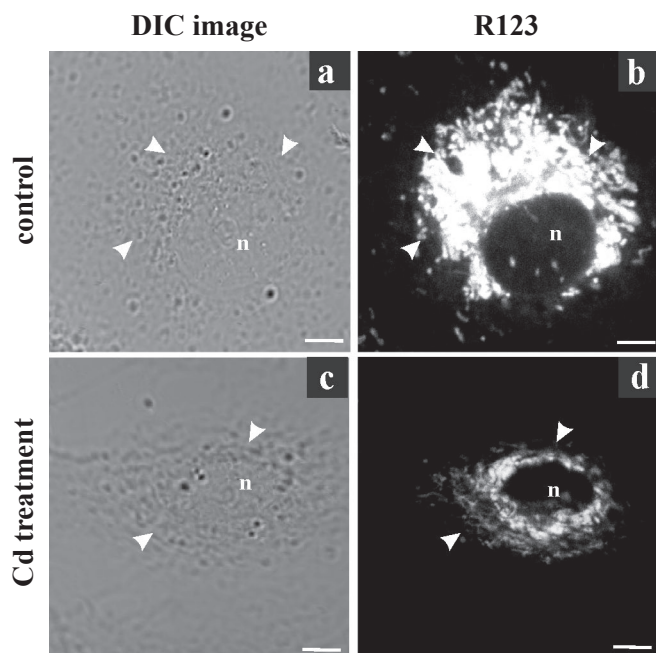


FIGURE 6. Differential interference contrast microscopy (DIC) (a, c) and confocal laser scanning microscopy of HuH-7 cells stained with rhodamine 123 (R123) (10 $\mu\text{g}/\text{mL}$) (b, d). (a) Normal aspect of untreated cell. (b) Control cell with filamentous fluorescence spread in the cytoplasm, indicating the functional area of the mitochondria (arrowheads). (c) Cd treated cell (5 μM for 12 h). (d) Cd treated cell (5 μM for 12 h) with punctate fluorescence, suggesting loss of mitochondrial functionality (arrowheads). n = nucleus. Scale bar: 10 μm .

(Fig. 6d, arrowheads), suggesting the loss of mitochondrial function in Cd treated cells. These results agree with the evidence from the MTT assay (Fig. 1b) and occurred in cells that remain attached following Cd treatment (5 μ M/12 h), indicating that mitochondria are an early target in Cd toxicity.

While mitochondrial function was impaired after Cd exposure, the acidic compartments increased in frequency and size (Fig. 7a-d). This increase in acidic vesicles may correspond with increased abundance of lysosomes in the cytoplasm (Fig. 8a-d). Consequently, the cells changed from a punctate regular fluorescent staining (Fig. 7b, 8b) to an intense fluorescence pattern corresponding to acid structures in the cytoplasm (Fig. 7d, 8d arrowheads).

The presence of fluorescent acidic compartments or lysosomal vacuoles further suggests the possibility of intracellular autophagic digestion. To disclose the presence of autophagosomes during Cd treatment, the cells were incubated with MDC (Fig. 9). Untreated cells (Fig.

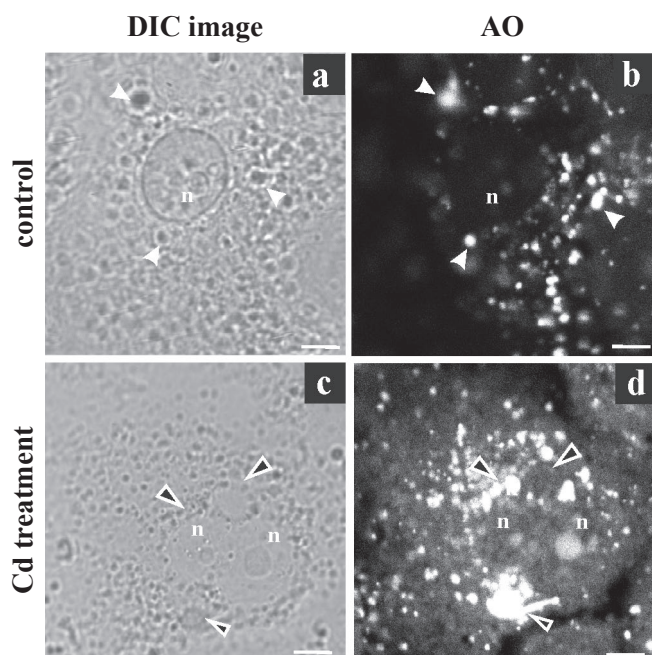


FIGURE 7. Differential interference contrast microscopy (DIC) (a, c) and confocal laser scanning microscopy of HuH-7 cells stained with acridine orange (AO) (5 μ g/mL) (b, d). (a) Control cell. (b) Untreated cell with punctate fluorescence staining in the cytoplasm corresponding to acidic organelles, such as endosomes and lysosomes (arrowheads). (c) Vacuolisation in Cd treated cells (5 μ M for 12 h) (arrow). (d) Intensely dispersed fluorescence observed in the cytoplasm (arrowheads) of treated cells (5 μ M for 12 h). n = nucleus. Scale bar: 10 μ m.

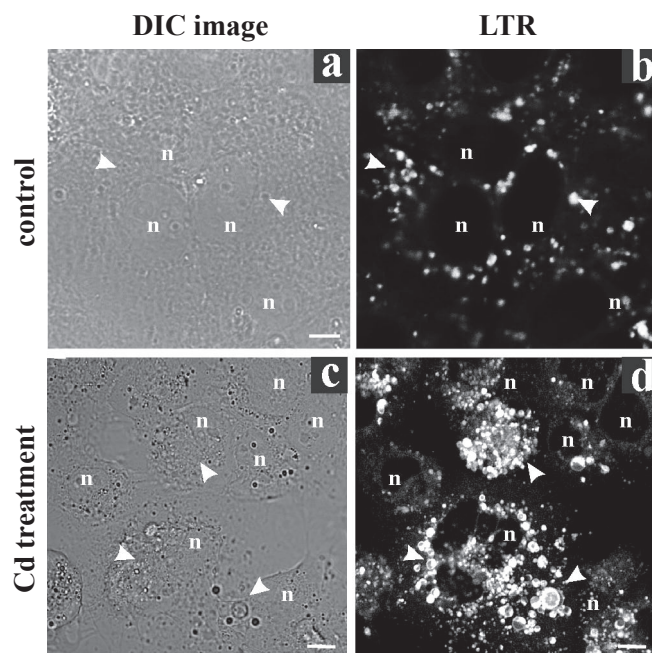


FIGURE 8. Differential interference contrast microscopy (DIC) (a and c) and confocal laser scanning microscopy of HuH-7 cells stained with LysoTracker Red (50 nM) (b and d). (a) Control cells. (b) Punctate fluorescence pattern observed in untreated culture (arrowheads). (c) Cd treated cell (5 μ M for 12 h). (d) Intense and dispersed fluorescence pattern indicate increased lysosomes throughout the cytoplasm (arrowheads). n = nucleus. Scale bar: 10 μ m (x400).

9a) exhibited no fluorescence indicative of autophagic vacuoles (Fig. 9b), while treated cells (Fig. 9c) showed a high frequency of fluorescent compartments and even the formation of large vacuoles (Fig. 9d). Therefore, these results strongly suggest that the apoptotic pathway and autophagic processes are involved in Cd induced cell death.

The endoplasmic reticulum, a major organelle involved in detoxification (Voeltz *et al.*, 2002), was analysed with the fluorescent dye DiOC₆ (Fig. 10). The dispersion of endoplasmic reticulum elements observed in untreated cells (Fig. 10a, b) changed after Cd treatment (Fig. 10c, d) even with the cell remaining adherent and spread (Fig. 10c).

Cytoskeleton microfilaments were also analysed for understanding the changes in cell structure after Cd treatment (Fig. 11). The extended microfilament network (Fig. 11b, arrowheads) changed after Cd treatment, given that the cells lost their microfilament projections in the cytoplasm (Fig. 11d, arrowheads) and their adhesion points on the substrates (Fig. 11d, arrowheads),

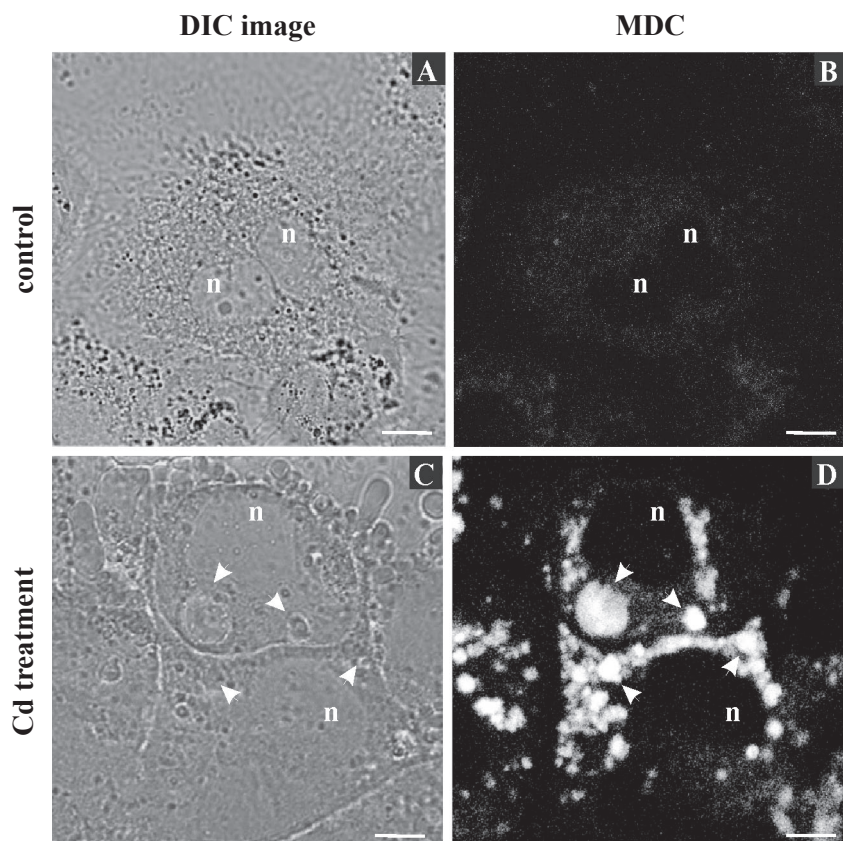
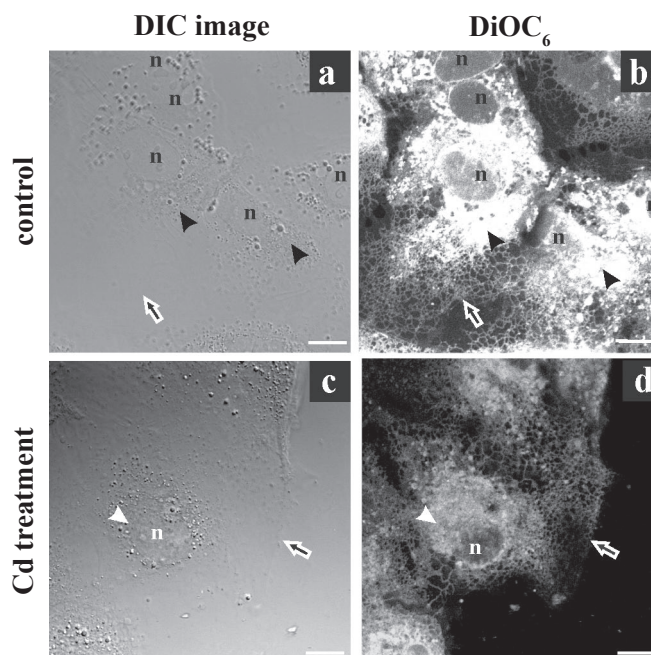


FIGURE 9. Differential interference contrast microscopy (DIC) (a and c) and confocal laser scanning microscopy of HuH-7 cells stained with monodansylcadaverine (MDC) (0.05 mM) (b and d) after Cd treatment (5 μ M for 12 h). (a) Control cells. (b) No fluorescence signal in untreated cells. (c) Cd treated cells with vacuoles in cytoplasm (arrowheads). (d) Autophagic vacuoles (arrowheads) staining in Cd treated cell indicating Cd mediated cell death through autophagic processes. n= nucleus. Scale bar: 10 μ m.

FIGURE 10. Differential interference contrast microscopy (DIC) (a, c) and confocal laser scanning microscopy of HuH-7 cells stained with DiOC₆ (2.5 μ g/mL) (b, d). (a) Control cells. (b) Morphological aspect of the reticular network of control cells with thinner peripheral regions (arrow) and regions with high fluorescence close to the nucleus, mainly because of the concentration of reticulum and other membranes, such as mitochondria (arrowheads) (c) Cd treated cells (5 μ M for 12 h). (d) Weaker fluorescence signal in treated cells (5 μ M for 12 h); with evidence of the disorganisation in reticular arrangement close to nucleus (arrowheads) and in cell periphery (arrow). n = nucleus. Scale bar: 10 μ m.



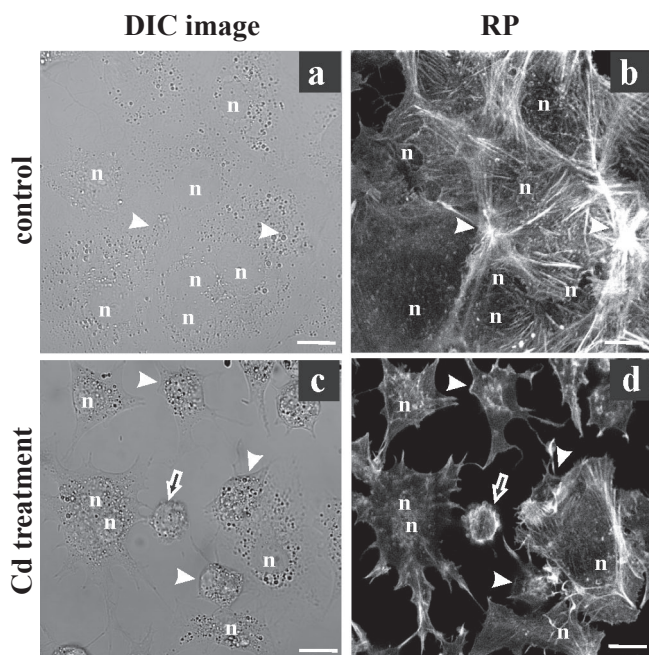


FIGURE 11. Differential interference contrast microscopy (DIC) (a, c) and confocal laser scanning microscopy of HuH-7 cells stained with rhodamine phalloidin (RP) (b, d). (a) Untreated cells in monolayer. (b) Extended of microfilament network and adhesion points (arrowheads) in control cells. (c) Cd treated cells (5 μ M for 12 h) displaying rounded morphology (arrow). (d) Loss of microfilament projections in the cytoplasm and of the adhesion points (arrowheads) in Cd treated cells (5 μ M for 12 h). n = nucleus. Scale bar: 10 μ m.

leading to an alteration in cell morphology (Fig. 11c, d, arrow).

Interestingly, multiple Cd induced damages in organelles were observed in treated cells that remained attached, indicating that the severity of the effect in different targets is important in inducing cell death. Therefore, Cd reached several targets at the same time leading to loss of mitochondrial function, endoplasmic reticulum dysfunction, cytoplasmic acidification and microfilament disorganisation. These processes are all occurring together in treated cells, and if the exposure is not halted, might lead to cell death by apoptotic and autophagic pathways.

Discussion

The results obtained clearly show that Cd induces a decrease in cell viability and progressive damage to cell morphology in HuH-7 cells through concurrent effects in multiple intracellular targets, including mi-

tochondria, cytoskeleton, endoplasmic reticulum and acidic compartments, leading to cell death through the apoptotic and autophagic pathways.

Apoptosis is considered a normal housekeeping event, but it is also necessary to arrest abnormal cell proliferation in development (Pulido and Parrish, 2003). Apoptosis can also be induced by a variety of chemicals, including many toxic metals (Rana, 2008), and is a known pathway of Cd mediated cell death (Wang *et al.*, 2009; Lasfer *et al.*, 2008; Ye *et al.*, 2007; Mao *et al.*, 2007; Pulido and Parrish, 2003; Faverney *et al.*, 2004). However, the present study indicates that apoptosis is not the only process observed in Cd treated cells, given that the autophagic pathway was also observed after sustained Cd exposure.

The autophagic pathway allows the digestion of dysfunctional organelles with resulting recirculation and reuse of their molecular constituents (Templeton and Liu, 2010). Furthermore, when Cd induced cell damage exceeds the repairing capacity of repair, cell death occurred. Dying cells generate increasing amounts of autophagic vacuoles and clear large proportions of their cytoplasm before dying (Bursch *et al.*, 2008).

The induction of Cd toxicity (cell death) in culture was asynchronous, suggesting preferential interference in some stages of the cell cycle. In fact, Cd can lead to cell cycle arrest, which may affect several cellular processes including cell proliferation and differentiation (Hartwig, 2010; Bertin and Averbeck, 2006). G2/M phase arrest was demonstrated after Cd exposure (Bork *et al.*, 2010), preventing damaged cells from entering into mitosis, until DNA damage is repaired. Therefore, some stages of the cell cycle might be more susceptible to Cd damage as suggested by the effect on different cells in the same culture.

Other authors have shown the isolated involvement of mitochondria (Caninno *et al.*, 2009), cytoskeleton (L'Azou *et al.*, 2002), endoplasmic reticulum (Wang *et al.*, 2009) and lysosomes (Lekube *et al.*, 2000) demonstrating the role of separate organelles and structures in Cd induced cell death. The present study shows that these intracellular targets are all being affected concurrently and contribute to cell dysfunction leading to cell death. Moreover, the present study shows that the extent of damage induced by Cd treatment is eventually so severe that cells cannot reverse the toxic effects as shown by the 10 μ M treatment for 12 h in the reversibility test.

The present study has increased our understanding of the cellular mechanisms of Cd toxicity on HuH-7 cells, by showing the progression of Cd induced damage in cells, and the involvement of mitochondria,

lysosomes, acidic compartments, cytoskeleton and endoplasmic reticulum as targets of Cd toxicity. Further investigations should be addressed to show the effects of this metal on each of these organelles.

Acknowledgments

This work was supported by Fundação Carlos Chagas Filho de Amparo à Pesquisa do Estado do Rio de Janeiro (E-26/171.315/2004) (E-26/ 100.470/2007) (E-26/110.921/2008).

References

- Barak LS, Yocum RR, Nothnagel EA, Webb WW (1980). Fluorescence staining of the actin cytoskeleton in living cells with 7-nitrobenz-2-oxa-1,3-diazole-phalloidin. *Proceedings of the National Academy of Sciences (USA)* **77**: 980-984.
- Bertin G, Averbeck D (2006). Cadmium: cellular effects, modifications of biomolecules, modulation of DNA repair and genotoxic consequences (a review). *Biochimie* **88**: 1549-1559.
- Biederbick A, Kern HF, Elsasser HP (1995). Monodansylcadaverine (MDC) is a specific *in vivo* marker for autophagic vacuoles. *European Journal of Cell Biology* **66**: 3-14.
- Bork U, Lee WK, Kuchler A, Dittmar T, Thévenod F (2010). Cadmium-induced DNA damage triggers G2/M arrest via chk1/2 and cdc2 in p53-deficient kidney proximal tubule cells. *American Journal of Physiology - Renal Physiology* **298**: 255-265.
- Bursch W, Karwan A, Mayer M, Dornetshuber J, Fröhwein U, Schulte-Hermann R, Fazi B, Sano FD, Piredda L, Piacentini M, Petrovski G, Fésüs L, Gerner C (2008). Cell death and autophagy: Cytokines, drugs, and nutritional factors. *Toxicology* **254**: 147-157.
- Cannino G, Ferruggia E, Luparello C, Rinaldi AM (2009). Cadmium and mitochondria. *Mitochondrion* **9**: 377-384.
- Fabbri M, Urani C, Sacco MG, Procaccianti C, Gribaldo L (2012). Whole genome analysis and microRNAs regulation in HepG2 cells exposed to cadmium. *Altex* **29**: 2-12.
- Faverney CR, Orsini N, Sousa G, Rahmani R (2004). Cadmium-induced apoptosis through the mitochondrial pathway in rainbow trout hepatocytes: involvement of oxidative stress. *Aquatic Toxicology* **69**: 247-258.
- Filipič M (2012). Mechanisms of cadmium induced genomic instability. *Mutation Research* **733**: 69-77.
- Fotakis G, Cemeli E, Anderson D, Timbrell J (2005). Cadmium chloride-induced DNA and lysosomes damage in hepatoma cell line. *Toxicology in vitro* **19**: 481-489.
- Hartwig A (2010). Mechanisms in cadmium-induced carcinogenicity: recent insights. *Biometals* **23**: 951-960.
- Idziorek T, Estaquier J, De Bells F, Ameisen JC (1995). YO-PRO-1 permits cytofluorometric analysis of programmed cell death (apoptosis) without interfering with cell viability. *Journal of Immunological Methods* **185**: 249-258.
- Joseph P (2009). Mechanisms of cadmium carcinogenesis. *Toxicology and Applied Pharmacology* **238**: 272-279.
- Johnson LV, Walsh ML, Chen LB (1980). Localization of mitochondria in living cells with rhodamine 123. *Proceedings of the National Academy of Sciences (USA)* **77**: 990-994.
- Kielian MC, Cohn ZA (1980). Phagosome-lysosome fusion. *Journal of Cell Biology* **85**: 54-765.
- Lasfer M, Vadrot N, Aoudjehane L, Conti F, Bringuier AF, Feldmann G, Reyl-Desmars F (2008). Cadmium induces mitochondria-dependent apoptosis of normal human hepatocytes. *Cell Biology and Toxicology* **24**: 55-62.
- L'Azou B, Dubus I, Courtès CO, Labouyrie JP, Perez L, Pouvreau C, Juvet L, Cambar J (2002). Cadmium induces direct morphological changes in mesangial cell culture. *Toxicology* **179**: 233-245.
- Lekube X, Cajaraville PM, Marigomez I (2000). Use of polyclonal antibodies for the detection of changes by cadmium in lysosomes of aquatic organisms. *The Science of Total Environment* **247**: 201-212.
- Mao WP, Ye JL, Guan ZB, Zhao JM, Zhang C, Zhang NN, Jiang P, Tian T (2007). Cadmium induces apoptosis in human embryonic kidney (HEK) 293 cells by caspase-dependent and independent pathways acting on mitochondria. *Toxicology in vitro* **21**: 343-354.
- Mosmann T (1983). Rapid colorimetric assay for cellular growth and survival: application to proliferation and cytotoxicity assays. *Journal of Immunological Methods* **65**: 55-63.
- Nordberg G (2009). Historical perspectives on cadmium toxicology. *Toxicology and Applied Pharmacology* **238**: 192-200.
- Plantin-Carrenard E, Bringuier A, Derappe C, Pichon J, Guillot R, Bernard M, Foglietti MJ, Feldmann G, Aubery M, Braut-Boucher F (2003). A fluorescence microplate assay using yopro-1 to measure apoptosis: Application to HL60 cells subjected to oxidative stress. *Cell Biology and Toxicology* **19**: 121-133.
- Pulido MD, Parish AR (2003). Metal-induced apoptosis: Mechanisms. *Mutation Research* **533**: 227-241.
- Rana SVS (2008). Metals and apoptosis: Recent developments. *Journal of Trace Elements in Medicine and Biology* **22**: 262-284.
- Siu ER, Mruk DD, Porto CS, Cheng CY (2009). Cadmium-induced testicular injury. *Toxicology and Applied Pharmacology* **238**: 240-249.
- Souza V, Bucio L, Ruiz MCG (1997). Cadmium uptake by a human hepatic cell line (WRL-68 cells). *Toxicology* **120**: 215-220.
- Templeton DM, Liu Y (2010). Multiple roles of cadmium in cell death and survival. *Chemical Biological Interactions* **188**: 267-275.
- Terasaki M, Song J, Wong JR, Weiss MJ, Chen LB (1984). Localization of endoplasmic reticulum in living and glutaraldehyde-fixed cells with fluorescent dyes. *Cell* **38**: 101-108.
- Voeltz GK, Rolls MM, Rapoport, TA (2002). Structural organization of the endoplasmic reticulum. *EMBO Reports* **3**: 944-950.
- Waisberg M, Joseph P, Hale B, Beyersmann D (2003). Molecular and cellular mechanisms of cadmium carcinogenesis. *Toxicology* **192**: 95-117.
- Wang SH, Shih YL, Lee CC, Chen WL, Lin CJ, Lin YS, Wu KH, Shih CM (2009). The role of endoplasmic reticulum in cadmium-induced mesangial cell apoptosis. *Chemical Biological Interactions* **181**: 45-51.
- Ye JL, Mao WP, Wu AL, Zhang NN, Zhang C, Yu YJ, Zhou L, Wei CJ (2007). Cadmium-induced apoptosis in human normal liver L-02 cells by acting on mitochondria and regulating Ca²⁺ signals. *Environmental Toxicology and Pharmacology* **24**: 45-54.